Toward resolution-independent dust emissions in global models: Impacts on the seasonal and spatial distribution of dust

D. A. Ridley,[1] C. L. Heald,[1] J. R. Pierce,[2] and M. J. Evans[3]

Received 4 February 2013; revised 19 March 2013; accepted 22 March 2013; published 14 June 2013.

[1] Simulating the emission of mineral dust and sea-salt aerosol is nonlinear with surface winds and therefore requires accurate representation of surface winds. Consequently, the resolution of a simulation affects emission and is often corrected with nonphysical scaling in coarse resolution global models. We examine the resolution dependence of emissions in the GEOS-Chem model and find that globally, annual emissions at 4° × 5° resolution are 59% of those simulated at 2° × 2.5° and only 33% of emissions at 0.25° × 0.3125°. The spatial and seasonal distribution of dust emissions vary substantially, indicating that applying a uniform scaling is inappropriate. We demonstrate the benefit of characterizing the subgrid surface wind as a Weibull probability distribution, reconciling much of the difference in emissions between resolutions for dust. Such a representation is shown to have little impact on sea-salt emissions. **Citation:** Ridley, D. A., C. L. Heald, J. R. Pierce, and M. J. Evans (2013), Toward resolution-independent dust emissions in global models: Impacts on the seasonal and spatial distribution of dust, *Geophys. Res. Lett.*, *40*, 2873–2877, doi:10.1002/grl.50409.

1. Introduction

[2] Mineral dust contributes significantly to many aspects of climate and atmospheric chemistry through scattering and absorbing radiation (*Forster et al*., 2007), by providing surfaces for heterogeneous reaction of trace gases (e.g., *Hanisch et al*., 2003) and by deposition of nutrients to the biosphere (e.g., *Swap et al*., 1992). Therefore, dust emissions must be adequately represented in global climate and chemical transport models. These models generally have coarse horizontal resolutions of over 100 km but the factors influencing the emissions (e.g., surface wind speeds) may not be homogeneous over these distances. Observational studies are providing new information on dust emission processes, and their microphysical properties (e.g., *Marsham et al*., 2012) and high-resolution regional simulations (on the order of km) have been undertaken to model the complex meteorological processes that drive convective dust events (*Heinold et al*., 2013); however, this level of information cannot be routinely applied in large-scale models. It is therefore essential to understand how necessary simplifications impact the simulation of dust in large-scale models and whether higher fidelity simplifications can be developed.

[3] The resolution of a simulation will affect the result for processes that have a nonlinear dependence on meteorological fields, such as wind-driven aerosol emission. This can be expressed with the following inequality,

$$\overline{u^n} \neq \bar{u}^n, \tag{1}$$

where u is a nonuniform array and n is any number other than 1. In terms of dust emission, which scales to the third power of near-surface wind speed, the calculated emission flux will change as a function of model resolution owing to the variability in subgrid wind speed. Previously, this problem has been accounted for by applying a uniform global scaling factor to the emissions (*Zender et al.*, 2003).

[4] Most dust emission parameterizations also require a wind threshold to be exceeded, above which saltation commences as suggested by observational studies (*Kok et al*., 2012). This threshold can bias coarse model simulations which apply a single mean wind speed to the entire model grid box. We illustrate this by considering the parameterization used in the Dust Entrainment and Deposition (DEAD) scheme (*Zender et al.*, 2003),

$$F_d = \begin{cases} \dfrac{\alpha c_s \rho u_*^3}{g}\left(1-\dfrac{u_{*t}}{u_*}\right)\left(1+\dfrac{u_{*t}}{u_*}\right) & : u_* > u_{*t} \\ 0 & : u_* \leq u_{*t} \end{cases} \tag{2}$$

where the vertical dust flux, F_d, is a function of frictional wind speed (u_*), threshold frictional wind speed (u_{*t}), the sand blasting efficiency (α), air density (ρ), acceleration due to gravity (g), and c_s is a constant (2.61) determined from wind tunnel tests (*White*, 1979). For any frictional wind speed below the threshold frictional wind speed, no dust will be emitted for the entire model grid box. In reality, if the mean wind is close to the threshold, we would anticipate that at some locations within the grid box, the wind will exceed the threshold and dust production will occur.

[5] We explore two possible solutions to the resolution dependence of the emissions: (1) to treat u_*^3 as a separate variable when averaging the high-resolution winds to coarser resolutions addressing the inequality expressed above ("cubed wind") and (2) to represent the grid box wind with a probability distribution accounting for emission when the mean wind is below the threshold ("wind PDF").

2. Methodology

[6] We use v9-01-01 of the GEOS-Chem model (www.geos-chem.org) driven by GEOS-5 meteorology for November 2011 to October 2012 and 10-m surface winds derived from the

[1]Department of Civil and Environmental Engineering, Massachusetts Institute of Technology, Cambridge, MA, USA.
[2]Department of Atmospheric Science, Colorado State University, Fort Collins, CO, USA.
[3]National Center for Atmospheric Science / Department of Chemistry, University of York, York, UK.

Corresponding author: D. A. Ridley, Department of Civil and Environmental Engineering, Massachusetts Institute of Technology, Cambridge, MA, USA. (daridley@mit.edu)

0094-8276/13/10.1002/grl.50409

Table 1. The Dust Emissions (As a Percentage of Those Produced at 0.25° × 0.3125°) Are Displayed for Each Resolution of 10-m Wind Fields, Assuming a Threshold Wind Speed of 5 ms^{-1} in the Offline Dust Model[a]

Dust Emissions	Standard	Cubed Wind	Wind PDF
Resolution (Degrees)	(%)	(%)	(%)
0.25 × 0.3125	100	100	100
0.5 × 0.67	85 ± 2	86 ± 2	88 ± 1
1 × 1.25	77 ± 5	81 ± 6	87 ± 2
2 × 2.5	**57 ± 8**	**64 ± 10**	**77 ± 3**
4 × 5	**33 ± 10**	**40 ± 12**	**64 ± 3**

[a]The range for a ±1 ms^{-1} change in the assumed threshold wind speed for dust uplift is indicated. The six simulations that are performed online are highlighted in bold.

latest 0.25° × 0.3125° GEOS 5.7.2 meteorology, here called "high-resolution winds". We use the DEAD dust emissions module (*Zender et al.*, 2003) and the dust source map derived from topography and TOMS aerosol index (*Ginoux et al.*, 2001; *Prospero et al.*, 2002). The frictional wind speed is derived from the 10-m wind speed, and the threshold wind speed is calculated based on the soil moisture, air density, and clay fraction (fixed at 0.2 globally) following *Zender et al.* (2003). Dust optical properties rely on the Global Aerosol Data Set with improvements to the UV/visible refractive indices (*Sinyuk et al.*, 2003) and an updated submicron dust distribution (*Ridley et al.*, 2012). The standard model dust emissions total 1085 Tg yr^{-1} in 2012 at 2° × 2.5° resolution.

[7] The probability distribution for surface wind speeds can be represented by a Weibull distribution and has been shown to hold for the scales considered in this study (*Cakmur et al.*, 2004). From *Justus et al.* (1978) equations (1) and (13), we derive the Weibull distribution in nondimensional form,

$$p\left(\frac{u}{\bar{u}}\right) = k\Gamma\left(1+\frac{1}{k}\right)\left\{\frac{u}{\bar{u}}\Gamma\left(1+\frac{1}{k}\right)\right\}^{k-1} e^{-\left\{\frac{u}{\bar{u}}\Gamma\left(1+\frac{1}{k}\right)\right\}^{k}} \quad (3)$$

$$\frac{\sigma}{\bar{u}} = \sqrt{\frac{\Gamma\left(1+\frac{2}{k}\right)}{\left[\Gamma\left(1+\frac{1}{k}\right)\right]^2} - 1} \quad (4)$$

[8] The shape of the distribution is represented by a shape parameter, k, dependent on the instantaneous (u) mean $\bar{u}$ and the standard deviation (σ) of the wind, with $\Gamma\left(1+\frac{1}{k}\right)$ representing a gamma function. Using the first and second moments for a Weibull distribution, we solve for k by fitting a curve to the resulting relationship between $\frac{\sigma}{U}$ and k in equation (4). The high-resolution winds are used to derive u and σ within a grid box at each of the resolutions tested. Due to strong gradients in wind between land and ocean, we mask all ocean grid boxes during averaging. The 0.25° × 0.3125° winds are unlikely to capture all the subgrid variability; therefore, we apply a minimum standard deviation of 0.5 ms^{-1} (dust emission totals are relatively insensitive to the minimum standard deviation). The wind statistics are calculated offline and online integration of the dust flux over the wind PDF results in a negligible model runtime increase (<1%).

[9] We first simulate dust flux in an offline version of the dust module for the standard, cubed wind, and wind PDF parameterizations and for all five resolutions (Table 1). The offline dust model is a simplified version of the DEAD dust scheme in GEOS-Chem, allowing calculation of dust flux at any resolution but using a globally constant wind threshold and no snow cover. The 4° × 5° source map and meteorology are used for all resolutions so that only the 10-m wind changes between resolutions. To investigate the impact of resolution on spatial and seasonal dust emissions and aerosol optical depth (AOD), the GEOS-Chem model is run at 4° × 5° and 2° × 2.5° resolution for a full year using each parameterization (including a variable wind threshold).

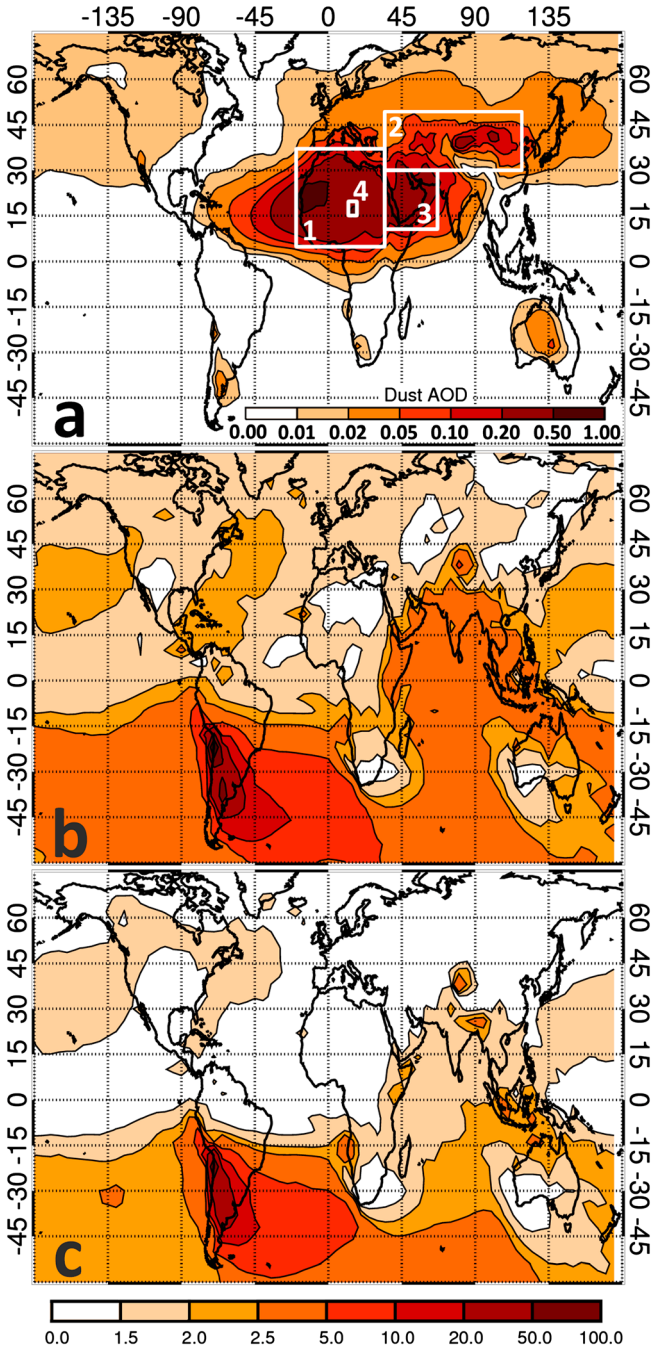

Figure 1. (a) The annual mean dust AOD is shown (note the log scale on the inset). The fractional difference between the dust AOD produced at 4° × 5° and 2° × 2.5° resolution is shown for the (b) standard parameterization and the (c) wind PDF parameterization. The seasonality of emissions in boxed regions is shown in Figure 3.

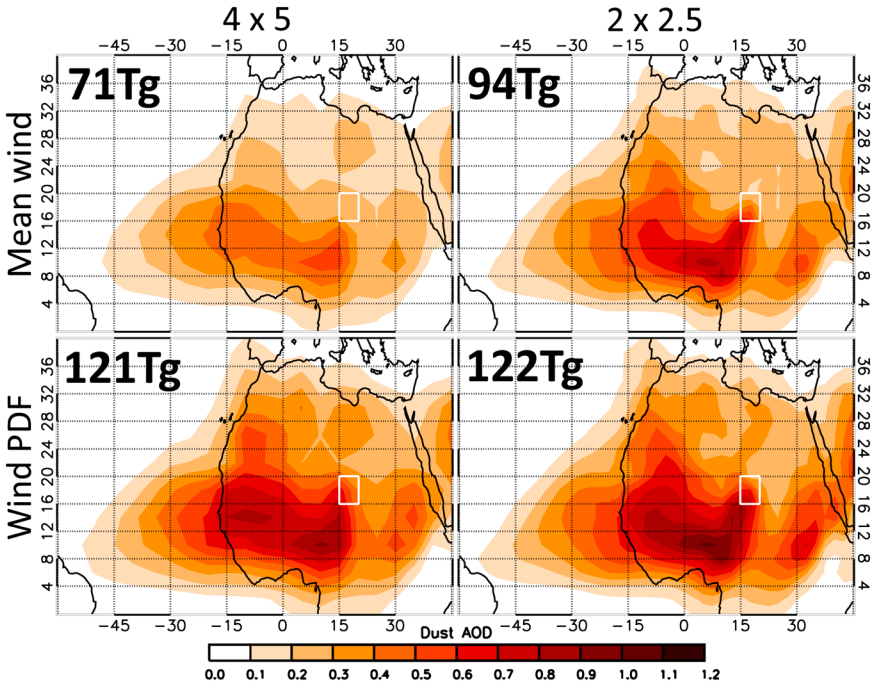

Figure 2. The GEOS-Chem dust AOD over Africa for March 2012 is shown for (left) 4° × 5° and (right) 2° × 2.5° resolutions and for (top and bottom, respectively) both the standard and wind PDF simulations. Total monthly dust emissions for North Africa are displayed, and the Bodélé Depression is marked with the white rectangle.

3. Results

[10] For the standard simulation, offline global dust emissions decrease rapidly with resolution, amounting to only 33% and 57% for 4° × 5° and 2° × 2.5° resolution, relative to the emissions generated using the high-resolution winds (Table 1). While the cubed-wind approach reduces this resolution dependence, the 4° × 5° simulation is still only able to account for 40% of the high-resolution emissions due to the wind threshold required for emission. By using the wind PDF, this increases to 64% and results in a marked decrease in the resolution dependence, bringing the emissions from the 4° × 5° simulation within 17% of the 2° × 2.5° emissions. Comparing the online 4° × 5° and 2° × 2.5° simulations, we find including the wind PDF produces a marked decrease in the resolution dependence of the dust AOD across the globe, particularly in high-dust regions such as Africa, resulting from increased emissions in the 4° × 5° simulation (Figure 1). In South America (contributing 2% of the global emissions), the discrepancy in emissions between resolutions is due to strong gradients in soil moisture, which increase the wind threshold, and cannot be captured at coarse resolution. A third of the global dust emissions occur when the mean wind speed is less than the wind threshold for dust uplift—emissions that are not captured by the cubed-wind simulations.

[11] Figure 2 illustrates the spatial differences in AOD between simulations over Africa for March. Much of the AOD results from dust emitted in the Bodélé Depression (indicated by the white rectangle) and transported south-west. The wind PDF increases emissions for both the 4° × 5° and 2 × 2.5° resolution simulations in this region, with the former changing more dramatically. This reduces the bias in March emissions between the two resolutions from 1.55 to 1.00 in the Bodélé Depression and from 1.32 to 1.01 over North Africa, improving agreement in AOD. This is notable as the Bodélé Depression produces almost 20% of the simulated annual African dust aerosol and is difficult to resolve in global models (*Washington et al*., 2009).

[12] Figure 3 shows the monthly dust emissions for regions that collectively emit over 95% of global dust emissions. We find year-round improvement in agreement between resolutions when using the wind PDF and observe that the seasonality of dust emissions is altered relative to the standard simulation. The emissions bias is reduced from a factor of 1.74 to 1.15 in Asia, and in the Middle East, the seasonality in monthly AOD is brought into better agreement (from $R^2 = 0.80$ using the standard simulation to $R^2 = 0.90$ using the wind PDF). In North Africa, the winter (October to March) emissions are 50% higher than summer (April to September) at 4° × 5° and only 21% higher at 2° × 2.5° when using the standard simulation. The wind PDF increases emissions in summer relative to winter giving more consistent seasonality between resolutions (17% and 12% higher in winter than summer for 4° × 5° and 2° × 2.5°, respectively). The GEOS-Chem simulation at 2° × 2.5° is capable of representing most observed features in the seasonality of African dust AOD from AERONET, MODIS, and MISR (*Ridley et al*., 2012). However, that study highlighted the underrepresented Bodélé Depression emissions and consistently low AOD in late summer relative to observations (and subsequently poor agreement with Barbados surface concentrations during this period)—both of these increase when using the wind PDF.

3.1. Implications for Sea-Salt Emissions

[13] Sea-salt emissions are also nonlinearly dependent on surface wind speeds. The GEOS-Chem simulation of

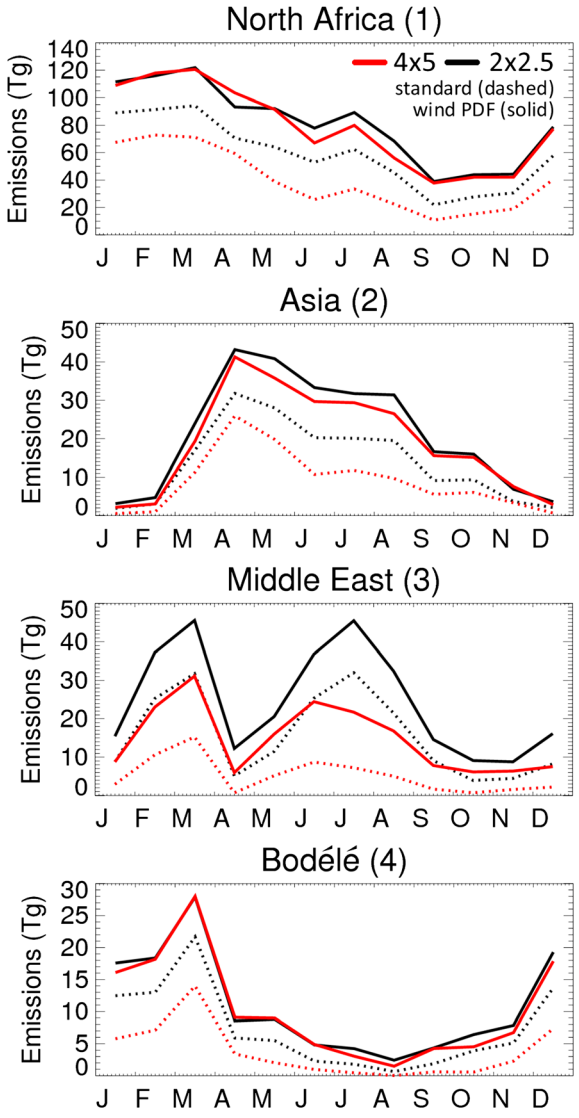

Figure 3. Modeled monthly mineral dust emissions for four regions are displayed for the standard (dashed line) and wind PDF (solid line) simulations at 4° × 5° (red) and 2° × 2.5° (black) resolutions. The region numbers correspond to the areas in Figure 1, and the Bodélé region (4) is a subset of the North Africa region (1).

sea-salt emissions is based on *Gong* (2003) with updates from *Jaegle et al*. (2010). As with mineral dust, we calculate the sea-salt emissions at 4° × 5° and 2° × 2.5° resolution, using the mean 10-m wind, the high-resolution wind to the power 3.41 (called "U341 field") and using the wind PDF.

[14] The total global emissions using 2012 surface winds are 3290 Tg yr^{-1} for the 2° × 2.5° simulation, approximately half of which are produced in the Southern Ocean (below 30 S). Monthly emissions at 4° × 5° are 6–9% lower globally. This is relatively small compared to the resolution dependence of dust because wind speeds exhibit lower subgrid variability over the oceans and emissions are spread over a wide area rather than from point sources. Very little seasonal or spatial dependence of sea-salt emission on resolution is seen in any region. Using the U341 field increases the total emissions for 4° × 5° and 2° × 2.5° by 9% and 4%, respectively, bringing agreement between simulations to within 3%. We expect this remaining difference to be a consequence of the temperature dependence of emissions (*Jaegle et al*., 2010).

[15] We also test the application of a wind speed threshold, suggested to range between 3 and 5 ms^{-1} by *Lewis and Schwartz* (2004) and find only a 0.2% decrease in the total global emissions for a 4 ms^{-1} threshold, indicating that this is regularly exceeded. These results suggest that using no wind threshold for sea-salt emission in global models is a reasonable simplification. We conclude that, unlike mineral dust emissions, sea-salt emissions are relatively independent of model resolution.

4. Conclusions

[16] We have shown that the magnitude, spatial distribution, and seasonality of dust emission depends upon the resolution of the global model. Preserving the higher-order wind field (i.e., u^3 for dust) when averaging from high-resolution data is not as effective at removing the resolution dependence as using a Weibull distribution. This is a consequence of significant dust emission occurring when the mean wind is less than the threshold for saltation. The Weibull distribution reconciles much of the difference in emission flux between model resolutions, increasing 4° × 5° global dust emissions from 59% to 84% of those at 2° × 2.5° resolution. Without adequate representation of subgrid winds, model resolution alters the seasonality and spatial distribution of emissions, especially in North Africa. Incorrect seasonality of African dust emissions in coarse resolution climate models is likely to impact their ability to simulate changes in the temperature of the atmosphere and the Atlantic sea surface. This has implications for adequately representing the Atlantic Meridional Mode and therefore hurricane genesis (e.g., *Evan et al*., 2011).

[17] The uniform soil texture and surface roughness assumed in the model will reduce the sensitivity to land surface properties. Fidelity of dust emission may benefit from better representation of these properties and consideration of their subgrid distribution, e.g., soil moisture that can follow a power law distribution (*Rodriguez-Iturbe et al*., 1995). Also, dust emissions from convective processes (e.g., Haboobs) are not well captured in coarse resolution simulations; additional parameterizations may be necessary to adequately represent these sources of dust aerosol in global models.

[18] While we have focused on aerosol emission, the choice of model resolution has been shown to affect other processes within global models, for example, secondary organic aerosol production (*Wainwright et al*., 2012) and estimation of the direct radiative effect via hygroscopic growth of aerosol (*Bian et al*., 2009). Reconciliation of differences due to model resolution may be realized for other processes within global models by using a similar approach as this study. While high-resolution simulations may be necessary for some applications, this study illustrates that using a simple representation of subgrid properties in a global model yields sensible results at coarse resolution and for relatively little computational expense.

[19] **Acknowledgments.** The authors thank R. Lucchesi and M. Karki at GMAO for providing the GEOS-5 data, and M. Hobby and J. Marsham for useful discussions.

References

Bian, H., M. Chin, J. M. Rodriguez, H. Yu, J. E. Penner, and S. Strahan (2009), Sensitivity of aerosol optical thickness and aerosol direct radiative effect to relative humidity, *Atmos. Chem. Phys.*, *9*, 2375–2386, doi:10.5194/acp-9-2375-2009.

Cakmur, R. V., R. L. Miller, and O. Torres (2004), Incorporating the effect of small-scale circulations upon dust emission in an atmospheric general circulation model, *J. Geophys. Res. Atmos.*, *109*, doi:10.1029/2003JD004067.

Evan, A. T., G. R. Foltz, D. Zhang, and D. J. Vimont (2011), Influence of African dust on ocean–atmosphere variability in the tropical Atlantic, *Nat. Geosci.*, *4*, doi:10.1038/NGEO1276.

Forster, P., et al. (2007), *Changes in Atmospheric Constituents and in Radiative Forcing, Climate Change 2007: The Physical Science Basis. Contribution of Working Group I to the Fourth Assessment Report of the Intergovernmental Panel on Climate Change*, Cambridge University Press, Cambridge, United Kingdom and New York, NY, USA.

Ginoux, P., M. Chin, I. Tegen, J. M. Prospero, B. Holben, O. Dubovik, and S.-J. Lin (2001), Sources and distributions of dust aerosols simulated using the GOCART model, *J. Geophys. Res.*, *106*, 20,255–20,273.

Gong, S. (2003), A parameterization of sea-salt aerosol source function for sub- and super-micron particles, *Global Biochem. Cycles*, *17*, 1097, doi:10.1029/2003GB002079.

Hanisch, F., and J.N. Crowley (2003), Ozone decomposition on Saharan dust: an experimental investigation, *Atmos. Chem. Phys.*, *3*, 119–130, doi:10.5194/acp-3-119-2003.

Heinold, B., P. Knippertz, J. Marsham, S. Fiedler, N. S. Dixon, K. Schepanski, B. Laurent, and I. Tegen (2013), The Role of Deep Convection and Nocturnal Low-Level Jets for Emission in Summertime West Africa - Estimates from Convection-permitting Simulations, *J. Geophys. Res. Atmos.*, doi:10.1002/jgrd.50402.

Jaeglé, L., P. K. Quinn, T. S. Bates, B. Alexander, and J.-T. Lin (2010), Global distribution of sea salt aerosols: new constraints from in situ and remote sensing observations, *Atmos. Chem. Phys.*, *11*, 3137–3157, doi:10.5194/acp-11-3137-2011.

Justus, C. G., W. R. Hargraves, A. Mikhail, and D. Graber (1978), Methods for Estimating Wind Speed Frequency Distributions, *J. Appl. Meteorol.*, *17*, 350–353.

Kok, J. F., E. J. R. Parteli, T. I. Michaels, and D. B. Karam (2012), The physics of wind-blown sand and dust, *Rep. Prog. Phys.*, *75*, 106901, doi:10.1088/0034-4885/75/10/106901.

Lewis, R., and E. Schwartz (2004), Sea Salt Aerosol Production: Mechanisms, Methods, Measurements and Models—A Critical Review, *Geophys. Monogr. Ser. 152* doi:10.1029/GM152.

Marsham, J., et al. (2012), Meteorology and dust in the central Sahara: Observations from Fennec supersite-1 during the June 2011 Intensive Observation Period, *J. Geophys. Res. Atmos.*, doi:10.1002/jgrd.50211.

Prospero, J. M., P. Ginoux, O. Torres, S. E. Nicholson, and T. E. Gill (2002), Environmental characterization of global sources of atmospheric soil dust identified with the Nimbus 7 Total Ozone Mapping Spectrometer (TOMS) absorbing aerosol product, *Rev. Geophys.*, *40*, doi:10.1029/2000RG000095.

Ridley, D. A., C. L. Heald, and B. Ford (2012), North African dust export and deposition: A satellite and model perspective, *J. Geophys. Res.*, *117*, D02202, doi:10.1029/2011JD016794.

Rodriguez-Iturbe, I., G. K. Vogel, and R. Rigon (1995), On the spatial organization of soil moisture fields, *Geophys. Res. Lett.*, *22*, 2757–2760.

Sinyuk, A., O. Torres, and O. Dubovik (2003), Combined use of satellite and surface observations to infer the imaginary part of refractive index of Saharan dust, *Geophys. Res. Lett.*, *30*, doi:10.1029/2002GL016189.

Swap, R., M. Garstang, S. Greco, R. Talbot, and P. Kallberg (1992), Saharan Dust in the Amazon Basin, *Tellus Ser. B-Chem. Phys. Meteorol.*, *44*, 133–149.

Wainwright, C. D., J. R. Pierce, J. Liggio, K. B. Strawbridge, A. M. Macdonald, and R. W. Leaitch (2012), The effect of model spatial resolution on Secondary Organic Aerosol predictions: a case study at Whistler, BC, *Canada. Atmos. Chem. Phys.*, *12*, doi:10.5194/acpd-12-16025-2012.

Washington, R., et al. (2009), Dust as a tipping element: the Bodele Depression, Chad, *Proc. Natl. Acad. Sci.*, *106*, doi:10.1073/pnas.0711850106.

White, B. R. (1979), Soil Transport by Winds on Mars, *J. Geophys. Res.*, *84*.

Zender, C. S., H. S. Bian, and D. Newman (2003), Mineral Dust Entrainment and Deposition (DEAD) model: Description and 1990s dust climatology, *J. Geophys. Res. Atmos.*, *108*, doi:10.1029/2002JD002775.